Appl. Phys. B 72, 677–683 (2001) / Digital Object Identifier (DOI) 10.1007/s003400100552

Applied Physics B
Lasers
and Optics

Properties of CdF_2:Ga as a medium for real-time holography

R.A. Linke[1], A.S. Shcheulin[2], A.I. Ryskin[2], I.I. Buchinskaya[3], P.P. Fedorov[3], B.P. Sobolev[3]

[1] NEC Research Institute, Inc., 4 Independence Way, Princeton, NJ 08540, USA
[2] S.I. Vavilov State Optical Institute, 12 Birghevaya Line, 199034 St Petersburg, Russia
[3] Crystallography Institute, 59 Leninskii Prospect, 117333, Moscow, Russia

Received: 20 November 2000/Published online: 20 April 2001 –

Abstract. The metastable nature of the excited state of bistable Ga centers in semiconducting CdF_2 crystals allows for the use of CdF_2:Ga and CdF_2:Ga, Y crystals as materials for real-time holography over a wide range of response times (1–1000 ms). The characteristics of these materials and optimal conditions for their use are discussed in the framework of a model that describes the decay of photo-induced gratings written in them.

PACS: 42.40.My; 42.70.Ln; 78.20.Bh

CdF_2:Ga is the most promising representative of the new class of holographic materials in which a photo-induced change in the density of bistable (DX center) states in a semiconductor crystal produces a local change of its refractive index (see [1, 2] and references therein). The excited state of the DX center has a metastable nature, being separated from the ground state by a potential barrier due to a strong lattice relaxation in the latter state [3–5]. Therefore, photo-induced gratings in such crystals are principally dynamic ones; their decay is determined by the height of the barrier and by the crystal temperature, T. Among crystals of this class, CdF_2:Ga has the highest barrier ~ 1 eV [2]. Thus, photo-induced metastable centers in this crystal are stable below ~ 200 K, as are the gratings formed by these centers. This stability allows for the use of CdF_2:Ga for static storage of information at $T < 200$ K [6]. At higher T the gratings are dynamic. In this paper we consider the mechanism of holographic grating decay in CdF_2:Ga and CdF_2:Ga, Y crystals. It is shown that at $T > 300$ K these crystals exhibit desirable properties for dynamic 3D holography for temporal changes in the frequency range of ~ 1–1000 Hz. Estimates of their important parameters and conditions for their use are given.

1 Sample preparation and mechanism of its photochromic nature

The CdF_2 crystals under investigation were grown from a melt using the Stockbarger–Bridgeman technique; dopants were added to the raw material. Due to a large difference in the ionic radii of Cd^{2+} and Ga^{3+}, the concentration of the active dopant ions does not exceed the relatively low value of 0.7×10^{18} cm^{-3} [2]. The extra charge (+1) of these ions is compensated by interstitial F^- ions, which is typical for the column-III impurities in fluoride crystals with a fluorite structure [7]. Together with these defects, randomly distributed over the crystal, are also impurity–fluorine clusters embedded in the lattice, also typical for fluorite-type crystals doped with the above impurities [8–10]. To convert the crystals into a semiconducting state they were annealed in a reducing atmosphere of K plus Cd vapor (a process called additive coloration). In this procedure, F^- ions diffuse from the volume of the crystal to the surface, and charge neutrality is maintained by a corresponding inward flow of electrons. These electrons reside at Ga ions or in the conduction band and thus convert the crystal into a semiconducting state [11]. However, this procedure does not result in the total depletion of F^- ions from the crystal, which inevitably contains a residual F^- concentration comparable to the concentration of impurities [10]. This is likely due to a dynamic interaction between clusters and isolated defects during the annealing (coloration) process. Therefore, the concentration of randomly distributed optically and electrically active Ga ions is given by

$$N_{\mathrm{Ga}} = n^* + N_{\mathrm{F}}\,, \tag{1}$$

where n^* and N_{F} are the concentrations of electrons introduced into the crystal during its coloration and residual F^- ions statistically distributed in the colored crystal, respectively. The relationship (1) shows that, in the ionic CdF_2 semiconductor, interstitial fluorine ions play the same role as acceptors in conventional semiconductors: they effectively decrease the concentration of donors, i.e. partly compensate them [12]. As is shown in [10], typically, $N_{\mathrm{F}} = (0.5 - 0.9)N_{\mathrm{Ga}}$.

At $T < 200$ K all electrons introduced into the crystal during coloration are associated with Ga ions, in pairs, forming the deep Ga centers (Ga^{1+}). It was shown in [2] that photo-induced conversion of bistable Ga centers from the two-electron ground ('deep') state into the metastable donor

state ($Ga^{3+} + e_{hydr}$, the 'shallow' state, where e_{hydr} denotes an electron localized at the hydrogenic orbital centered on the Ga^{3+} ion), in accordance with the reaction

$$Ga^{1+} + Ga^{3+} + h\nu \rightarrow 2(Ga^{3+} + e_{hydr}) \quad (2)$$

results in a noticeable change of the refractive index of the crystal, δn. This change creates the opportunity of writing phase holograms in the spectral gap between the photo-ionization absorption bands of the deep and shallow centers; these bands are located in the ultraviolet–visible (UV–VIS) and infrared (IR) ranges of the spectrum, respectively, and the gap covers a major portion of the visible range (Fig. 1). The refractive-index change results from the transition of tightly bound electrons of the deep centers into the loosely bound hydrogenic or free state. Accordingly, δn is proportional to the shallow donor center concentration, N_{sh}^0 (see [2], (8)). (Here and below the upper index in concentrations indicates the sign of the center with respect to the cation.) The $\delta n(\lambda)$ dependence within the gap was discussed in [2] in terms of a two-oscillator model with the high-frequency effective oscillator being responsible for the constant (spectrally independent) shift in δn and the low-frequency effective oscillator determining the quadratic character of this dependence (see [2], (4)). It seems natural to associate these oscillators with the photo-ionization absorption bands of the deep and shallow centers, respectively. Kramers–Kronig analysis shows that the photo-induced IR band is, in fact, responsible for at least 50% of the low-frequency effective oscillator.[1] The remaining contribution, if any, is possibly due to an increase of the lattice IR absorption (impurity-induced transitions) occurring at the change in the center state.

Along with singly doped CdF_2:Ga, crystals of CdF_2:Ga co-doped with Y were also studied. It was shown in [13, 14] that co-doping with Y increases the concentration of the optically active Ga and simultaneously significantly improves the optical quality of the crystal. Figure 1 shows the spectra of additively colored CdF_2:Ga and CdF_2:Ga, Y crystals at $T = 77$ K as-cooled in the dark and also after strong illumination in the UV–VIS band. One can see the very strong impurity absorption but also a *non-photochromic* UV–VIS absorption in the former sample and its reduced presence in the latter crystal. In addition to non-photochromic absorption, CdF_2:Ga crystals also show strong light scattering, which is stronger than the scattering from non-doped crystals by 4 orders of magnitude. Co-doping with Y decreases this scattering by ~ 2 orders of magnitude [13, 14]. However, the presence of Y also produces the objectionable effect of increasing IR absorption, with a tail that stretches into the VIS range of the spectrum. This absorption diminishes part of the incident radiation which contributes to the photochromic (deep-to-shallow conversion) process, i.e. it effectively lowers the quantum yield, $\mu = 2$, of this process [15, 16]. Thus, the Y concentration should be high enough to increase as much as possible the active Ga content in the crystal and low enough to minimize the additional IR absorption. This ideal concentration was found to result from $(0.015 - 0.020)$ mole % of YF_3 in the raw material. For these crystals, $N_{Ga} = 1.7 \times 10^{18}\,cm^{-3}$, which is the maximum active Ga concentration in CdF_2 achieved to date. The concentration of the randomly distributed (optically and electrically active) Y ions is not known. Based on the analysis of the absorption spectra of the crystals with the above Y content, we estimate this concentration to be $N_Y = (0.1 - 0.5)N_{Ga}$ [13].

Co-doping increases the concentration of electrons introduced into the crystal at coloration for two reasons: first, due to the increase of N_{Ga} and second, because of the additional quantity N_Y. At $T < 200$ K all the electrons are localized at the deep Ga centers. At photo-excitation of the crystal n^* electrons fill the hydrogenic orbitals at $(N_{Ga} + N_Y - N_F)$ impurity ions and form shallow Ga and Y centers. The characteristics of both centers (their binding energies, cross-sections for electron capture, Stokes shifts, etc.) are similar, though not identical. The distribution of electrons between N_{Ga} and N_Y impurity centers in such crystals is, in general, not known.

[1] It was concluded in [2] that the photo-induced IR band is not the main contributor to the low-frequency effective oscillator. However, (6) of [2] is incorrect. Using the corrected formula $\Delta n(\nu_1) = \frac{c}{2\pi^2}\int_0^\infty \frac{\Delta\alpha(\nu)d\nu}{\nu^2-\nu_1^2}$, where $\Delta\alpha$ is the photo-induced change of the absorption coefficient, we find the result quoted here.

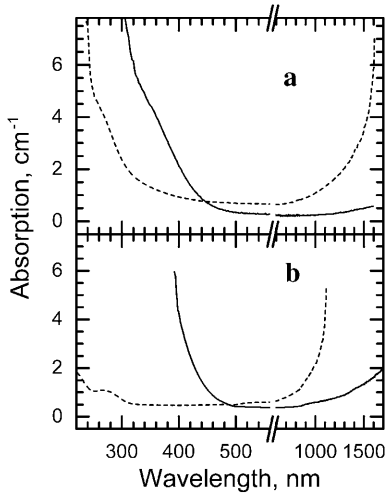

Fig. 1a,b. Absorption spectra of CdF_2:Ga (**a**) and CdF_2:Ga, Y (**b**) crystals cooled in the dark to $T = 77$ K (*solid lines*) and after UV–VIS illumination (*dashed lines*). Only the short-wavelength tail of the IR band is seen (for this band $\lambda_{max} \approx 7\,\mu m$)

2 Holographic gratings and mechanism of their decay

Some features of writing of holographic gratings in CdF_2:Ga are considered in [2]. The diffraction efficiency, $DE = \eta$, of the gratings increases as the square of the exposure fluence for weak exposures, then saturates and decreases with a further increase of the fluence due to scattering into the dark nodes of the grating ([2], Fig. 6). A peak DE of 0.92 was obtained at a total exposure of $0.3\,J/cm^2$ at $T = 100$ K, for which total deep–shallow center conversion is possible [17]. This is a relative DE, which is converted into an absolute efficiency by multiplying by the sample transmittance (normally, $0.5 - 0.7$ after the exposure). The sensitivity of grating writing was derived from the initial portion of the dependence of the diffraction efficiency on the exposure fluence using the Kogelnik relationship for a simple sinusoidal grating with

amplitude n_1:

$$\eta = \sin^2\left(\frac{\pi n_1 d}{\lambda_0 \cos\theta}\right), \tag{3}$$

where the refractive index is assumed to be spatially modulated in the form $n(x) = n_0 + n_1 \sin(x)$; $|n_1| = \delta n/2$. In (3) d is the grating thickness, λ_0 is the read-out wavelength in vacuum, and θ is the angle between the read-out beam and the normal to the grating surface. For not too large values of η this quantity depends essentially quadratically on δn. The dependence of writing sensitivity on the photon energy in eV, E ([2], Fig. 7), is closely fitted by an empirical expression $4.5 \times 10^{-16} \exp(E/0.133)$.

At $T > 200$ K the written hologram decays due to conversion of the photo-induced shallow centers in the antinodes of the grating into deep centers. This process proceeds until the equilibrium population of the shallow centers, characteristic of the crystal temperature, is achieved. This conversion is described by the reaction

$$2(N^0_{\rm sh} + e_{\rm hydr}) + kT \rightarrow N_{\rm d} + N^+_{\rm sh} \tag{4}$$

and includes the thermal release of an electron from the shallow donor center into the conduction band, its transport in the conduction band, and its capture by another shallow center with the subsequent formation of a deep center. The last stage also requires thermal activation due to the large lattice relaxation accompanying the deep-center formation (Fig. 2).

Balance equations for Ga centers and for electrons introduced into the crystal during coloration take the form:

$$N_{\rm Ga} = N^0_{\rm sh} + N^+_{\rm sh} + N_{\rm d} \tag{5}$$

and

$$n^* = N^0_{\rm sh} + 2N_{\rm d} + n\,, \tag{6}$$

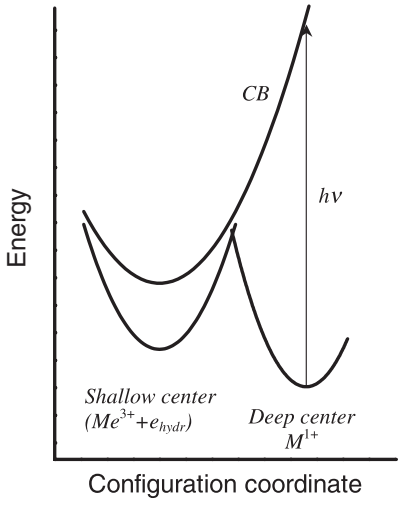

Fig. 2. Configuration diagram of the Ga center in CdF_2 showing the shift in configuration coordinate at the shallow-to-deep center conversion. 'CB' is the conduction band. Since the processes of shallow-to-deep and deep-to-shallow center conversion actually involve the transformation of *two* centers (two shallow centers or one deep center and one ionized shallow center) and two electrons they cannot be correctly described by a single-center configuration diagram which here has only illustrative value

respectively. Here, $N_{\rm d}$ and $N^+_{\rm sh}$ are the concentrations of the deep and ionized Ga centers, respectively, and n is the free-electron concentration. Both theoretical estimates and direct measurements of the conductivity of the crystals under investigation show that n in the actual temperature range of $(300-400)$ K does not exceed several percent of $N_{\rm Ga}$ (and $N_{\rm F}$, see above). With allowance for the 'compensation condition' (1) this means that the last term of (6) may, in practice, be neglected.

Taking account of (1), (5), and (6), the rate equation which describes the change with time of the shallow donor center concentration and includes the processes of thermal destruction (4) and formation as well as photo-induced formation (2) of these centers, may be written as:

$$\begin{aligned} {\rm d}N^0_{\rm sh}/{\rm d}t = &-\left(c - \frac{b}{4}\right)\left(N^0_{\rm sh}\right)^2 - \frac{b}{2} N_{\rm Ga} N^0_{\rm sh} \\ &+ \frac{b}{4}\left(N^2_{\rm Ga} - N^2_{\rm F}\right) + I\mu\sigma N_{\rm d}\,. \end{aligned} \tag{7}$$

Here, c and b are kinetics constants of the shallow-center thermal destruction and creation, respectively, I is the light intensity, and σ is the cross-section of photon absorption by the deep centers. This equation allows us to find, for finite T, the shallow-center concentration in the dark ($I = 0$) or under illumination of the crystal by light with intensity I, and the transient curves for transitions between these two cases.

Without specifying the details of the multi-stage process of thermal destruction of the shallow center (4), one may nevertheless propose that this process has a thermally activated nature, i.e. is characterized by an activation energy, $E^{\rm sh}_{\rm bar}$:

$$c(T) = \nu_1 \cdot \exp(-E^{\rm sh}_{\rm bar}/kT) \tag{8}$$

where ν_1 is a frequency factor. The same proposal is valid for the process of thermal destruction of the deep center:

$$b(T) = \nu_2 \cdot \exp(-E^{\rm d}_{\rm bar}/kT)\,. \tag{9}$$

$E^{\rm sh}_{\rm bar}$ and $E^{\rm d}_{\rm bar}$ may be considered as effective heights of the barriers separating the shallow state from the deep state and *vice versa*.

Equation (7) is identical in its structure to the rate equation found in [15] under the assumption that additive coloration results in the total removal of F^- ions from the crystal. This means that taking account of these ions (see (1)) does not change the pattern of the shallow-center decay after switching off the light; *it changes only the values of the equilibrium concentrations*. This pattern has the following appearance:

$$N^0_{\rm sh}(t) = n_2 + \frac{n_2 - n_1}{\exp\left[(t + t_0)/\tau\right] - 1}\,. \tag{10}$$

Here, t_0 is an integration constant, $\tau = \frac{1}{(c - b/4)(n_2 - n_1)}$ is a parameter which describes the rate of decay, and n_1, n_2 are roots of the right-hand side of (7):

$$\begin{aligned} n_{1,2} = &-\frac{N_{\rm Ga}}{4m-1}\left(1 + \frac{2I\sigma}{bN_{\rm Ga}}\right) \mp \frac{1}{4m-1} \\ &\times \sqrt{\left(\frac{2Io}{b}\right)^2 + 4\frac{Io}{b}\left[N_{\rm F}(1-4m) + 4N_{\rm Ga}m\right] + N^2_{\rm F}(1-4m) + 4N^2_{\rm Ga}m} \end{aligned} \tag{11}$$

Here, $m = c/b$ is the ratio of kinetics constants characterizing the thermal decay of shallow and deep centers. The n_2 root is equal to the equilibrium concentration of the shallow donor centers in the dark. It is shown in [15] that at $N_{\rm sh}^0 \ll N_{\rm Ga}$, $b \ll c$, i.e.

$$\tau \cong \frac{1}{c(n_2 - n_1)} . \tag{12}$$

Analysis of decay curves using (10) allows us to find the parameters n_2, $(n_2 - n_1)$, and τ.

For relatively high temperatures, when the constant b cannot be neglected, the expression for τ is more complex. Under the assumption that $N_{\rm F} < N_{\rm Ga}$ this expression can be written as follows:

$$\tau \cong \frac{1}{N_{\rm Ga}\sqrt{cb}} . \tag{13}$$

It is evident from (13) that an Arrhenius plot for τ allows one to find the quantity $\frac{1}{2}(E_{\rm bar}^{\rm sh} + E_{\rm bar}^{\rm d})$. Equation (12) has a smaller temperature range of applicability as compared with (13). A criterion for its use for the treatment of experimental data is an absent (or weak) dependence of n_2 on T, indicating a low rate of thermal decay of the deep center.

Thus, the shallow-center decay is described by the hyperbolic-cotangent-type dependence of (10). It is evident from (10) that this dependence converts to a simple exponential for $(t + t_0) \gg \tau$, and this inequality is satisfied either at the final stages of the decay (large t), or at higher temperatures (large n_2, i.e. small τ).

One should note that the inequality $b \ll c$ does not mean that we may neglect terms in (7) containing b since this change would significantly modify the character of the decay: it would shift from hyperbolic-cotangent to purely hyperbolic.

In principle, the presence of a co-dopant (Y) changes the decay pattern even if the parameters characterizing both shallow centers are identical. However, it will be shown below that the decay of shallow centers in CdF_2:Ga, Y follows (10) very closely.

3 Experimental study of grating decay

Two techniques were used for the experimental study of the decay problem: (i) measurement of the photo-induced IR absorption, which is a direct measure of $N_{\rm sh}^0$, and (ii) measurement of the DE of gratings written in the crystal; according to (3) the square root of this quantity is proportional to $N_{\rm sh}^0$ for moderate values of η (in practice, for $\eta \leq 0.7$). A 5-mm-thick CdF_2:Ga crystal was mounted in a variable-temperature cryostat and its transmissivity at $\lambda = 1.5\,\mu$m was measured as a function of time following a saturating exposure by a strong ($30\,{\rm mW/cm^2}$) beam at 476 nm. For the DE measurements, gratings were written into the sample using two interfering 476-nm beams and the DE was determined versus time by comparing the strengths of the transmitted and diffracted beams using an attenuated 476-nm beam as a probe. These measurements were repeated at several temperatures over the range of 240 to 300 K.

Figure 3 shows the decay of the optical density at $\lambda = 1.5\,\mu$m ($T = 254$ K) and the square root of DE of the grating for CdF_2:Ga ($T = 250$ K) together with fits to (10). One can see the near identity of the two decay curves and the high quality of the fits.

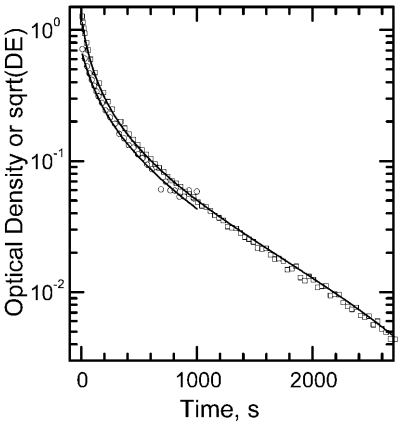

Fig. 3. The decay of photo-induced IR absorption ($\lambda = 1.5\,\mu$m, *open squares*) at 254 K and the square root of diffraction efficiency (*open circles*) at 250 K in CdF_2:Ga and their fits with (10) (*solid lines*)

Fitting decay patterns in the temperature range of $240\,{\rm K} < T < 300\,{\rm K}$ with (10) we find from an Arrhenius plot (Fig. 4) an activation energy for τ of (0.78 ± 0.05) eV. In this temperature range n_2 weakly depends on T (see below), therefore (12) is applicable. Determining $(n_2 - n_1)$ from the same fitting procedure, we find from (12) an activation energy for c, $E_{\rm bar}^{\rm sh} = (0.95 \pm 0.05)$ eV (see (8)).

Figure 5 shows decay curves for IR ($\lambda = 1.3\,\mu$m) absorption of a CdF_2:Ga, Y crystal of 2-mm thickness at $T = 293$ K and $T = 345$ K and their fits with (10). The fine fit for both temperatures (as well as for intermediate temperatures) shows that decay in the co-doped crystal obeys the same regularities as decay in CdF_2:Ga.

Figure 6 shows IR absorption of this crystal in the range of $(193 - 344)$ K in the dark and after illumination at 488 nm ($1.46\,{\rm W/cm^2}$). The 'dark' absorption is proportional to the n_2 root of (9). Below ~ 300 K, n_2 is small and depends only weakly on T, which justifies the use of (12) for finding $E_{\rm bar}^{\rm sh}$ in this range (see above). Its increase with T reflects the thermal population of the shallow donor levels. The $n_2(T)$ dependence is determined with (11) at $I = 0$ under the assumption $N_{\rm F} = 0$. This expression describes well the dark absorption in the range of (293 –

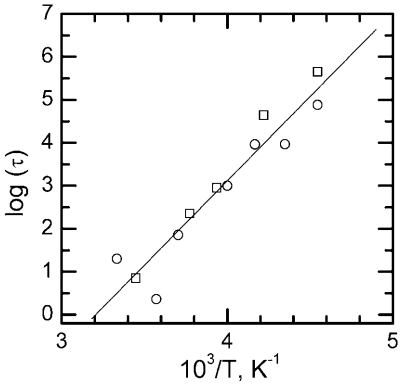

Fig. 4. An Arrhenius plot of data showing decay in IR absorption ($\lambda = 1.5\,\mu$m, *open squares*) as well as in the square root of diffraction efficiency (*open circles*) in CdF_2:Ga versus inverse temperature

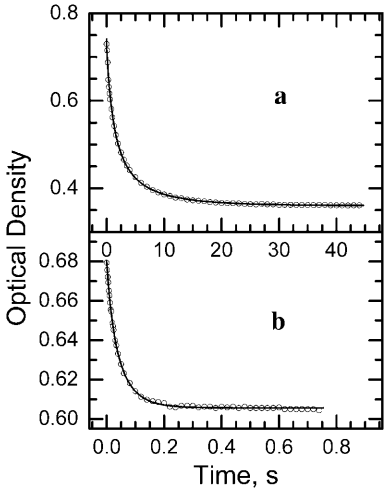

Fig. 5a,b. Decay of photo-induced IR absorption ($\lambda = 1.3\,\mu$m) in CdF_2:Ga, Y at 293 K (**a**) and 345 K (**b**). *Open circles* are experimental points, *solid lines* are fits with (10)

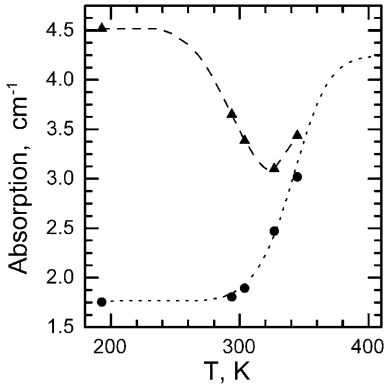

Fig. 6. Temperature dependence of IR absorption ($\lambda = 1.3\,\mu$m) in CdF_2:Ga, Y in the dark, which characterizes the equilibrium concentration of shallow centers (*black circles* are experimental points, *dotted line* is a calculation using (11)) and during photo-excitation by an argon-ion laser ($\lambda = 488$ nm, power 1.46 W/cm^2); *black triangles* are experimental points, *dashed line* shows the trend

344) K and one may assume that it applies also for higher temperatures.

The light-induced absorption at $T = 193$ K corresponds to total deep-to-shallow center conversion. Analysis of the low-temperature dependence of this absorption on illumination time (Fig. 7) shows that 46% conversion occurs at an exposure fluence of 0.45 J/cm^2. (Taking into account the two-times higher concentration of energy in antinodes of the grating, such conversion level ensures $0.92DE$ for a grating written with this laser in this crystal, see [17].) This value is near the experimental exposure fluence of 0.3 J/cm^2 for CdF_2:Ga (see above).

Figure 6 reveals that beginning at $T \sim 250$ K a total deep-to-shallow center conversion becomes impossible (at finite power density of the exciting light of 1.46 W/cm^2) due to thermal destruction of deep centers; this is the origin of the decrease of the equilibrium absorption under illumination with increased T (in the range of $(250-320)$ K). However, further increase of T results in an increase in absorption because of the growth in the equilibrium population of the shallow centers (n_2).

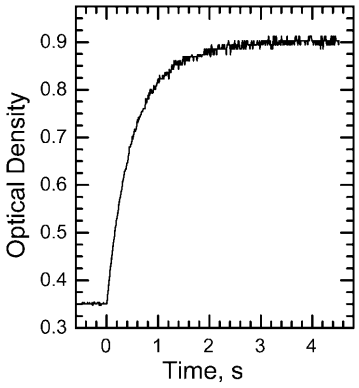

Fig. 7. Growth of IR absorption ($\lambda = 1.3\,\mu$m) in CdF_2:Ga, Y under illumination by an argon-ion laser ($\lambda = 488$ nm, power 1.46 W/cm^2). $T = 193$ K

For characterization of the crystal response for real-time holography, we assume that gratings are to be written with short pulses with sufficient energy to realize a total deep-to-shallow conversion during a time short compared with the decay time of the hologram. The highly local nature of holographic gratings using DX materials [18] makes the hologram decay essentially independent of the grating period over a wide range of spatial frequencies.

For reasonably fast response times and relatively strong gratings (conflicting requirements), we restrict our analysis to the temperature range of $(293-344)$ K, in which the decay of 1.3-μm absorption was studied. Figure 8 shows the $t_{0.1}$(IR) dependence on temperature in this range, where $t_{0.1}$(IR) is the time for a tenfold decrease of the photo-induced absorption of the shallow centers (as measured from the maximum initial absorption possible for this T) for the finite power of the exciting light. (One should note that, according to (3) for $\eta \leq 0.7$, a *tenfold* decrease in IR absorption corresponds to a *hundredfold* decrease in η, $\tau_{0.01}(DE)$). An Arrhenius plot of the $\tau(1/T)$ dependence gives an activation energy for τ of (0.84 ± 0.05) eV, in reasonable agreement with this quantity found for CdF_2:Ga (see above). In this range

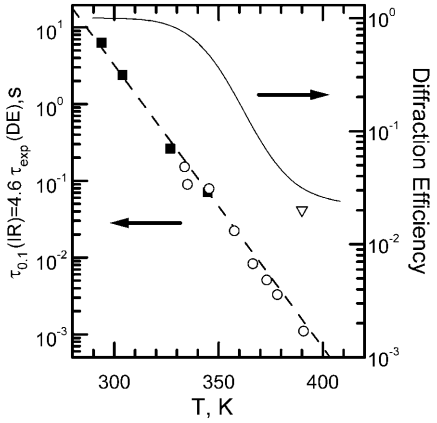

Fig. 8. Temperature dependence of (i) decay time of photo-induced IR absorption ($\lambda = 1.3\,\mu$m, *black squares*) and holographic gratings (square root of diffraction efficiency, *open circles*); the *dashed line* is the result of a calculation using (10) with an activation energy of 0.84 eV and (ii) initial (maximum) diffraction efficiency of the hologram for a given T calculated with (3) using the data of Fig. 6 (*solid line*) for a CdF_2:Ga, Y crystal with $d = 2$ mm. The *open triangle* shows an experimental value of DE for $T = 390$ K corrected for the crystal thickness

n_2 depends strongly on T; therefore (13) was used for determining the barrier characteristics. Using (13), we find from an Arrhenius plot of the $\tau(1/T)$ dependence $\frac{1}{2}(E^{\rm sh}_{\rm bar} + E^{\rm d}_{\rm bar}) = (0.84 \pm 0.05)$ eV and $E^{\rm d}_{\rm bar} = 1.68 - 0.95$ eV $= 0.73$ eV. This energy, corresponding to the thermal release of electrons to the conduction band, is equal to the binding energy of the deep center. This energy was found, in a first-principles calculation [19], to be 0.7 eV, in excellent agreement with the above $E^{\rm d}_{\rm bar}$ value.

One should stress the difference in physical meaning between the $E^{\rm sh}_{\rm bar}$ and $E^{\rm d}_{\rm bar}$ quantities. The shallow-to-deep conversion process includes two thermal-activation processes, which are combined in the $E^{\rm sh}_{\rm bar}$ barrier height: (i) release of an electron from the shallow center into the conduction band and (ii) its capture by the second shallow center, which requires a significant re-arrangement of the center ion positions. For Ga, the process (ii) gives the main contribution to $E^{\rm sh}_{\rm bar}$. The reverse process of the deep-to-shallow conversion happens after thermal release of the first of two electrons from the deep center into the conduction band, and this is the only process that contributes to the $E^{\rm d}_{\rm bar}$ barrier height.

We now analyze the temperature dependence of the diffraction efficiency (Fig. 8). The right-hand scale in Fig. 8 shows 'initial' DE (at the beginning of the decay), which corresponds to the stationary value of δn at finite T. To find the $\eta(T)$ dependence, the absorption data of Fig. 6 were used. The absorption, measured at $T = 193$ K, gives the maximum possible change of IR absorption which corresponds to the maximum possible change of the refractive index. This change was found to be equal, for this crystal, to 2.8×10^{-4} (at $\lambda = 514$ nm). With allowance for (3) one can find that for low-frequency gratings ($\cos\theta \approx 1$), the maximum value of the relative DE (~ 1) [20] can be achieved for crystals with $d \geq 2$ mm. The maximum absorption measured ($T = 193$ K) allows us to convert the photo-induced IR absorption (i.e. the change in absorption induced by UV–VIS illumination) at an arbitrary temperature into δn and, with the use of (3), into η. Let us emphasize that, according to the above assumption, under the conditions of this experiment, exciting light always results in a total deep-to-shallow conversion; however at $T \geq 300$ K, η decreases with increased T due to the increase in the equilibrium shallow-center concentration, $n_2(T)$, as calculated with (11) above.

The question arises as to the temperature dependence of the fluence necessary for writing of the maximum-strength grating (at finite T). Absorption at the writing/reading wavelength decreases with increased T due to the process of thermal destruction of deep centers, i.e. due to the decrease of their concentration. At wavelengths where the crystal is sufficiently transparent, the portion of the energy absorbed in the crystal will be linearly dependent on the equilibrium concentration of deep centers, and the fluence necessary for $\sim 46\%$ conversion of these centers, i.e. for writing of the strongest possible grating for this T (see above), will not depend on the temperature. As is shown above, this fluence is 0.45 J/cm^2.

In order to test the reliability of these estimates we performed experiments with direct writing of holograms in a CdF_2:Ga, Y crystal with $d = 10$ mm in the T range of $(330 - 390)$ K using a second-harmonic single-pulse Nd:YAG laser ($\lambda = 532$ nm). The pulse energy density at the sample was ~ 4 J/cm^2 and the pulse duration was 20 ns. Decay of holograms is nearly exponential in this temperature range; for such a decay $\tau_{0.01}(DE) \cong 4.6\tau_{\rm exp}(DE)$. We observed good agreement with decay times found in the absorption experiments. The maximum relative diffraction efficiency for $T = 390$ K was $\sim 20\%$, also in reasonable agreement with the calculated η value for this temperature (correcting for the sample thickness which was 5 times larger than that of the crystal for which absorption kinetics were studied).

Thus, Fig. 8 gives the essential holographic parameters for CdF_2:Ga, Y crystals with $d = 2$ mm for the writing of holograms with a laser ($\lambda = 514$ nm) with an energy density at the sample of ~ 0.5 J/cm^2, sufficient to realize a total deep-to-shallow conversion for times shorter than $\tau_{0.01}(DE)$. With allowance for (3) and the wavelength dependence $|\delta n| \sim \lambda^2$ in the spectral region of interest, this information is enough for a choice of the optimal sample thickness and necessary conditions for writing and reading of dynamic holograms with this type of crystal.

4 Conclusions

The metastable nature of the photo-induced state of the Ga centers in CdF_2:Ga and CdF_2:Ga, Y crystals allows the application of these crystals as materials for real-time holography over a wide range of response times, with temperature as the controlling parameter. A simple bimolecular model of the grating decay, despite many approximations, describes in adequate detail the decay process and the relevant characteristics of the materials.

Acknowledgements. The research described in this publication was made possible in part by Award No. RP1-2096 of the US Civilian Research & Development Foundation for the Independent States of the Former Soviet Union (CRDF) and by Grant No. 99-02-17871 of the Russian Foundation for Basic Research (RFBR). We are grateful to Ian Redmond and George Devlin for obtaining some of the experimental data reported here.

References

1. R.A. Linke, I. Redmond, T. Thio, D.J. Chadi: J. Appl. Phys. **83**, 661 (1998)
2. A.I. Ryskin, A.S. Shcheulin, E.A. Miloglyadov, R.A. Linke, I. Redmond, I.I. Buchinskaya, P.P. Fedorov, B.P. Sobolev: J. Appl. Phys. **83**, 2215 (1998)
3. D.J. Chadi, K.J. Chang: Phys. Rev. B **39**, 10 063 (1989)
4. J. Dabrowski, M. Scheffler: Mater. Sci. Forum 83–87, 735 (1992)
5. Two Ga DX centers were assumed to exist in CdF_2 ([2], also A.I. Ryskin, A.S. Shcheulin, D.E. Onopko: Phys. Rev. Lett. **80**, 2949 (1998)). It was shown, however, that effects ascribed to the second DX center in fact were due to the In contamination in CdF_2:Ga crystals (B. Koziarska-Glinka, A. Barcz, L. Arizmendi, A. Suchocki: Phys. Rev. B **61**, 9295 (2000))
6. R.A. Linke, I. Redmond, G. Devlin, A.I. Ryskin, A.S. Shcheulin: OSA Technical Digest Series, CLEO-2000 (2000) p. 188; I.R. Redmond, R.A. Linke, A.I. Ryskin, A.S. Shcheulin: Proc. 7th OSA Topical Meeting Opt. Comput. – Technical Digest (1999) pp. 100–102
7. W. Hayes (Ed.): *Crystals with the Fluorite Structure* (Clarendon, Oxford 1974)
8. S.A. Kazanskii: JETP Lett. **38**, 521 (1983); Sov. Phys. JETP **62**, 727 (1985); JETP Lett. **41**, 224 (1985)
9. J.P. Laval, A. Abaous, B. Frit, A. Le Bail: J. Solid State Chem. **85**, 133 (1990)
10. S.A. Kazanskii, D.S. Rumyantsev, A.I. Ryskin: in press
11. The analogous process happens at the coloration of CdF_2 crystals for a majority of the column-III dopants
12. CdF_2 is a monopolar semiconductor of n-type; hole conductivity is absent in this crystal

13. R.A. Linke, I. Redmond, A.I. Ryskin, A.I. Shcheulin, I.I. Buchinskaya, P.P. Fedorov, B.P. Sobolev, S. Ivanov: unpublished
14. Russian Patent No. 99119779/28 (020523)
15. A.S. Shcheulin, A.I. Ryskin, K. Swiatek, J.M. Langer: Phys. Lett. **222**, 107 (1996)
16. This value of μ was found experimentally for the CdF_2: In crystal. Determination of this quantity for CdF_2:Ga is hampered by the strong non-photochromic UV–VIS absorption in this crystal (see Fig. 1a)
17. Further increase of the exposure does not increase DE (up to $\eta = 1$) but, instead, reduces DE due to increasing action of the scattered light in nodes of the grating
18. The grating strength was found to be constant up to a grating period of 1 μm and decreases by 20% for smaller periods down to 0.1 μm for gratings written in GaAlAs:Si [1]
19. C.H. Park, D.J. Chadi: Phys. Rev. Lett. **82**, 113 (1999)
20. Actually, the maximum value of η equals 0.92 [2]